AGU PUBLICATIONS

Geophysical Research Letters

RESEARCH LETTER
10.1002/2017GL073140

Special Section:
Early Results: Juno at Jupiter

Jupiter gravity field estimated from the first two Juno orbits

W. M. Folkner[1], L. Iess[2], J. D. Anderson[3], S. W. Asmar[1], D. R. Buccino[1], D. Durante[2], M. Feldman[3], L. Gomez Casajus[5], M. Gregnanin[2], A. Milani[4], M. Parisi[1], R. S. Park[1], D. Serra[4], G. Tommei[4], P. Tortora[5], M. Zannoni[5], S. J. Bolton[3], J. E. P. Connerney[6], and S. M. Levin[1]

[1]Jet Propulsion Laboratory, California Institute of Technology, Pasadena, California, USA, [2]Dipartimento di Ingegneria Meccanica e Aerospaziale, Sapienza Università di Roma, Rome, Italy, [3]Southwest Research Institute, San Antonio, Texas, USA, [4]Dipartimento di Matematica, Università di Pisa, Pisa, Italy, [5]Dipartimento di Ingegneria Meccanica e Aerospaziale, Università di Bologna, Forlì, Italy, [6]NASA Goddard Space Flight Center, Greenbelt, Maryland, USA

Abstract The combination of the Doppler data from the first two Juno science orbits provides an improved estimate of the gravity field of Jupiter, crucial for interior modeling of giant planets. The low-degree spherical harmonic coefficients, especially J_4 and J_6, are determined with accuracies better than previously published by a factor of 5 or more. In addition, the independent estimates of the Jovian gravity field, obtained by the orbits separately, agree within uncertainties, pointing to a good stability of the solution. The degree 2 sectoral and tesseral coefficients, $C_{2,1}$, $S_{2,1}$, $C_{2,2}$, and $S_{2,2}$, were determined to be statistically zero as expected for a fluid planet in equilibrium.

Key Points:
- The Jupiter gravity field has been evaluated for the first two Juno orbits
- The zonal harmonics J_4 and J_6 improve over previous results by factors of 5 and 22, respectively, providing strong constraints on Jupiter interior models

Supporting Information:
- Supporting Information S1

Correspondence to:
W. M. Folkner,
william.m.folkner@jpl.nasa.gov

Citation:
Folkner, W. M., et al. (2017), Jupiter gravity field estimated from the first two Juno orbits, *Geophys. Res. Lett.*, *44*, 4694–4700, doi:10.1002/2017GL073140.

Received 17 FEB 2017
Accepted 2 MAY 2017
Published online 25 MAY 2017

1. Introduction

After about 5 years of cruise from Earth, the Juno spacecraft entered orbit around Jupiter on 5 July 2016. The orbit was nearly polar and highly eccentric with a period of 53 days. During each perijove, where the spacecraft was closest to Jupiter's center of mass, the spacecraft was within 1.06 of Jupiter's radius, where R_J = 71,492 km is Jupiter's equatorial radius at the 1 bar level derived from radio occultation measurements [*Lindal et al.*, 1981]. Two-way radio Doppler data were acquired during the few hours near perijove as a part of the Juno gravity science experiment. This paper presents the estimated gravity field obtained by processing the first two perijove data.

The main objective of the Juno gravity science experiment is to estimate the gravity field of Jupiter in order to provide constraints on models of the interior structure. Since the motion of the Juno spacecraft is perturbed by the gravity field of Jupiter, one can recover the gravity field by accurately tracking the motion of the spacecraft. Prior to the arrival of Juno, the best published gravity field of Jupiter was estimated from the Doppler measurements acquired by the Pioneer 10 and 11 [*Anderson et al.*, 1974; *Null et al.*, 1975] and Voyager 1 and 2 spacecraft [*Campbell and Synnott*, 1985]. These data provided estimates of the low-degree spherical harmonic coefficients as well as the mass and spin-pole direction of Jupiter.

The orbit geometry of Juno is much more sensitive to Jupiter's gravity field compared with previous spacecraft missions. Hence, from the first perijove alone, the accuracy of the recovered gravity field has substantially improved over the previous results. The second perijove provides further improvement in the accuracy of Jupiter's gravity field and the ability to test for possible systematic errors. Our results show that the accuracy of the gravity field coefficients has improved substantially. Especially, the J_4, J_6, and J_8 terms are improved by more than a factor of 5 compared with previously estimated values. The other estimated gravity coefficients (i.e., $C_{2,1}$, $S_{2,1}$, $C_{2,2}$, $S_{2,2}$, odd harmonic coefficients, and even harmonic coefficients with degree greater than 8) were also estimated, but the recovered values are statistically insignificant (i.e., less than the uncertainty).

2. Mission Orbit Geometry and Data

Key geometry information for the first two Juno perijoves following orbit insertion, designated PJ1 and PJ2, are given in Table 1. The orbit was nearly polar with orbit period 53 days. The time of perijove is given in barycentric dynamical time (TDB). The orbit plane was nearly perpendicular to the direction from Earth to Jupiter. Both perijoves were near solar conjunction. At perijove the height of the spacecraft above the 1 bar ellipsoid

Table 1. Geometry Information for Perijoves 1 and 2, Including Time of Perijove, One-Way Light Time LT From Spacecraft to Earth, Distance *d* From Juno to Earth, Inclination of Orbit Plane to Jupiter Equator, Height Above Jupiter 1 Bar Ellipsoid at Perijove, Latitude λ of Perijove, Angle β Between Orbit Normal and Direction From Earth to Jupiter, and Angular Separation SEP Between Sun and Jupiter as Seen From Earth

PJ	Time (TDB)	LT(min)	*d*(au)	*i*(deg)	*h*(km)	λ(deg)	β(deg)	SEP(deg)
1	27/08/2016 12:51:52	53.0	6.37	89.9	4147	3.8	2.8	22.6
2	19/10/2016 18:12:02	53.1	6.39	90.0	4179	4.7	9.4	18.2

was about 4100 km at latitude 3.8°N and 4.7°N. The spacecraft was nearly over the north pole of Jupiter about 1 h before perijove and above the south pole about 1 h after perijove. When above the north and south poles the spacecraft was approximately one Jupiter radius above the 1 bar level.

The data used for estimating the Jovian gravity field are measurements of the Doppler shift of the Juno radio signal by tracking stations of the NASA Deep Space Network. For PJ1 the data used were from 3.2 h before perijove to 5.1 h after perijove. For PJ2 the data were from 3.1 h before perijove to 2.8 h after perijove. For both perijoves, the tracking station transmitted a radio signal to the spacecraft at X band (8 GHz). A transponder on the spacecraft locked coherently in phase onto the signal from the tracking station and transmitted a signal back to the tracking station.

For PJ1 the spacecraft transmitted signals at both X band and at Ka band (32 GHz). The differences in the Doppler shift of the X-band and Ka-band signals were used to calibrate the effect of charged particles on the radio signal from the spacecraft to Earth. The only significant signature in this calibration was near the time of closest approach to Jupiter. Near perijove the spacecraft was inside the orbit of Io and the radio signal passed through the Io plasma torus. The Io plasma torus causes an effect on radio signals that has been previously measured from the Voyager and Ulysses spacecraft [*Eshleman et al.*, 1979; *Bird et al.*, 1992]. We used the dual-frequency radio signal to Earth to calibrate the effect of the plasma torus, also applied, appropriately scaled, to the X-band radio signal from the tracking station to the spacecraft. Figure 1 shows this calibration on the Doppler shift measured at the tracking station. For PJ2 the spacecraft transmitted only X band so no charged particle calibration data are available. We applied an estimate of the effect of the Io plasma torus to the PJ2 data based on the dual-frequency measurements from PJ1. Most future Juno perijove tracking data will use dual frequencies for both transmission to the spacecraft and transmission from the spacecraft to calibrate charged particle effects more completely.

For both perijoves Jupiter was relatively near solar conjunction. For this geometry the dominant noise on the Doppler data was expected to be caused by fluctuations in the integrated density of electrons emitted by the Sun (solar plasma) along the line from Earth to Jupiter [*Asmar et al.*, 2005]. However, at the observation times, the solar plasma fluctuations were smaller than expected. The measurement noise for the two orbits is characterized by the Allan deviation [*Barnes et al.*, 1971] that measures the fractional frequency stability as a function of the difference in time τ between pairs of measurements. The Allan deviation gives a measure of the noise as a function of time interval and is commonly used as an alternate to power spectral analysis. For the Jovian gravity field estimation the main time scales of interest are from ~100 s to ~1000 s, for which the change in Doppler is caused by the zonal gravity harmonics from degree 2 to degree 12. Figures 2 and 3 show the Allan deviation for Doppler residuals. These are based on

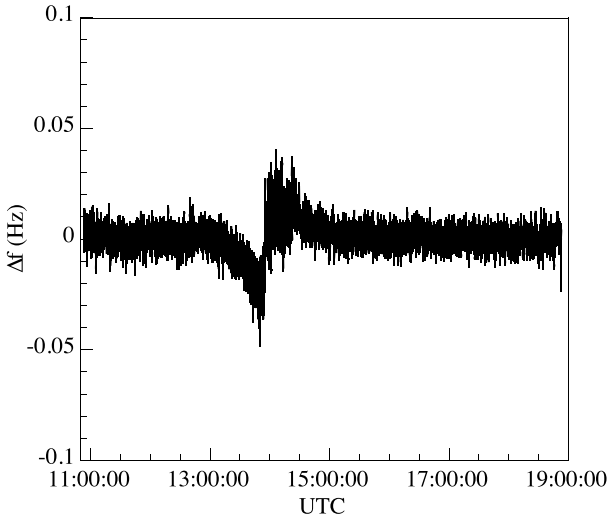

Figure 1. The correction to the X-band Doppler measurements for PJ1 on 27 August 2016 due to the effect of charged particles along the signal path from Juno to Earth, derived from the difference between the X-band and Ka-band measurements. The signature in the calibration near time of perijove was due to the Io plasma torus.

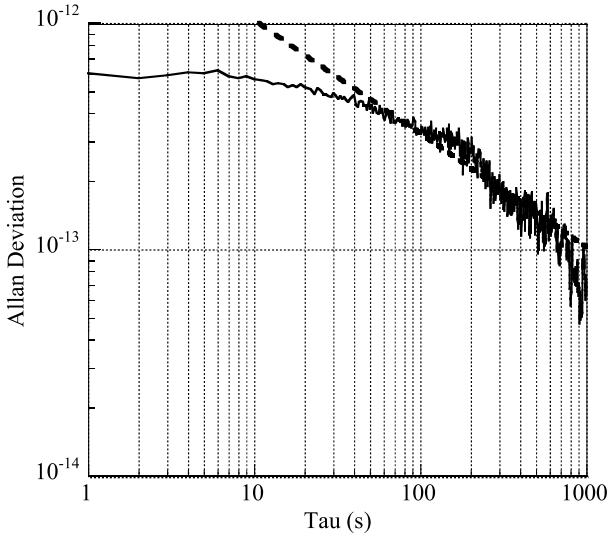

Figure 2. The Allan deviation of the Doppler measurements from PJ1. For time scales from 100 s to 1000 s the slope is approximately proportional to tau$^{-1/2}$ (dashed line) indicating that the Doppler measurements are independent for those time scale.

residuals after estimation of the relevant parameters. Data from the hour centered on perijove are excluded, since over that time the estimated parameters can absorb some of the measurement noise. Doppler data noise for planetary missions is often dominated by solar plasma that appears in the Allan deviation as a slope of $\tau^{-1/6}$ [*Woo et al.*, 1976]. When solar plasma noise is low, Doppler data noise is often dominated by fluctuations in the Earth troposphere that appears in the Allan deviation as a slope of $\tau^{-1/2}$ [*Keihm et al.*, 2004]. Our data processing software accommodates either of these two cases. We use the slope of the Allan deviation to see which of these two cases is a better approximation for the noise in each data arc. The slope of the Allan deviation for PJ1 residuals over 100 s to 1000 s indicates that the Doppler measurements are approximately uncorrelated, while for PJ2 the slope of the Allan deviation indicates noise dominated by solar plasma.

3. Model and Estimation Technique

The mass distribution of a planet is generally different from that of a homogeneous spherical body. The external gravitational potential of Jupiter can be conveniently expanded in series of spherical harmonics of degree n and order m [e.g., *Kaula*, 1966]:

$$U(r,\lambda,\varphi)=\frac{GM}{r}\left[1-\sum_{n=2}^{\infty}\left(\frac{R}{r}\right)^{n}J_nP_{n,0}(\sin\varphi)+\sum_{n=2}^{\infty}\sum_{m=1}^{n}\left(\frac{R}{r}\right)^{n}P_{n,m}(\sin\varphi)\left[C_{n,m}\cos(m\lambda)+S_{n,m}\sin(m\lambda)\right]\right],$$

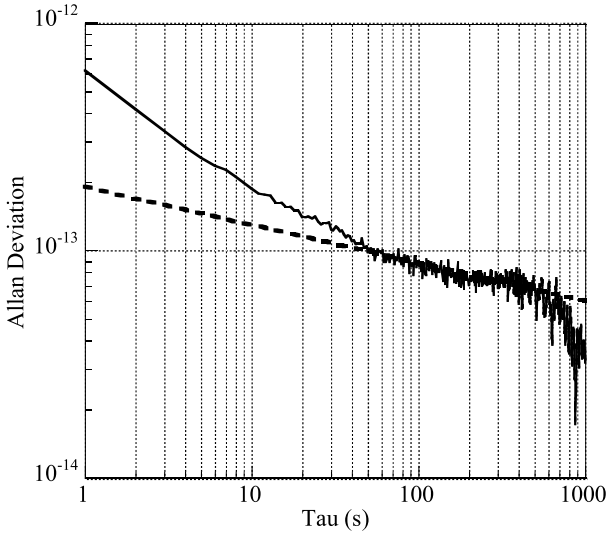

Figure 3. The Allan deviation of the Doppler measurements from PJ2. For time scales from 100 s to 1000 s the slope is approximately proportional to tau$^{-1/6}$ (dashed line) indicating that the Doppler measurements are correlated on those time scales due to the character of solar plasma.

where G is the gravitational constant, M and R are the mass and equatorial radius of Jupiter, r is the distance from Jupiter's center of mass, φ is the latitude, λ is the longitude, $P_{n,m}$ are the unnormalized associated Legendre functions, and $C_{n,m}$ and $S_{n,m}$ are the unnormalized spherical harmonic coefficients. The gravitational acceleration affecting the trajectory of Juno while orbiting about Jupiter can be calculated by taking the gradient of the gravitational potential. The spherical harmonic coefficients can be estimated, along with other relevant parameters, by measurements of the Doppler shift of the radio signal from the spacecraft.

Given a set of measurements z, it is possible to obtain a least squares estimate x_c for the set of the estimated parameters x, by combining the

measurements with a priori information [*Bierman*, 1977]:

$$x_c = \left(A^T W A + \widetilde{\Lambda}\right)^{-1}\left(A^T W z + \widetilde{\Lambda}\tilde{x}\right),$$

where A is the matrix of observation partials, W is the observable weighting matrix, $\widetilde{\Lambda}$ is the a priori information matrix, and $\tilde{x}$ is an unbiased a priori estimate of the state vector. The quantity P_x, given by

$$P_x = \left(A^T W A + \widetilde{\Lambda}\right)^{-1},$$

is the covariance matrix, which bears information about the estimation accuracies. The square roots of the diagonal elements correspond to the formal uncertainties on the estimated parameters.

The measurements used for gravity analysis allow the estimation of a limited number of parameters, supported by the available data strength. However, unestimated parameters (for instance, higher degree and order gravity harmonics) can be dynamically correlated with the estimated parameters and might undermine the estimated values and uncertainties.

One strategy to prevent the underestimation of the covariance is the technique of consider analysis. This approach features a set of parameters y which are not estimated, but whose a priori covariance P_y is used to augment the least squares uncertainty. The consider covariance P_{CON} is given by

$$P_{\mathrm{CON}} = P_x + S P_y S^T,$$

where S is the sensitivity matrix:

$$S = \partial(x - x_c)/\partial y$$

where $x - x_c$ is the difference between the true value of x and the least squares estimate x_c. The consider covariance is composed of two positive definite terms: (i) the formal covariance matrix P_x and (ii) an additional component which depends on the sensitivity matrix and the a priori covariance for the unestimated parameters.

When data are accumulated (i.e., data available for more than one perijove) they are possible to adopt a multiarc approach [*Milani and Gronchi*, 2010], where the information from different arcs is combined. In this case, the formal uncertainties P_x will decrease because of the higher information content, while the consider covariance P_{CON} can sometimes increase when estimated parameters are highly correlated with unestimated parameters.

4. Jovian Gravity Field Estimation

The Doppler data from PJ1 and PJ2 were used to estimate the Jovian gravity field parameterized by zonal harmonics through degree 12 and sectoral and tesseral harmonics of degree 2 along with corrections to the Jupiter spin axis direction and the initial position and velocity of the spacecraft for each perijove. Because Jupiter rotates 90° in ~2.5 h, data from each Juno perijove are sensitive to sectoral and tesseral harmonics of degree 2. The Juno data have less sensitivity to the Jupiter mass parameter (GM) than the data from the Galileo orbiter flybys of the Galilean satellites. We have applied a constraint to the Jupiter GM based on a fit to the Galileo orbiter data [*Jacobson et al.*, 1999]. The a priori uncertainties for the other estimated parameters were set to be large compared with the final estimated uncertainties. The Jovian gravity field is also affected by tides raised by the Jovian satellites, with largest contribution by Io. Because the longitude of Juno with respect to Io was almost the same for PJ1 and PJ2 the data are not able to separate the tide signature. Instead, we have modeled the effect of tides using a value for the k_2 Love number of 0.379 from *Gavrilov and Zharkov* [1977]. The tide model causes time-averaged corrections $\Delta J_2 = 0.054 \times 10^{-6}$ and $\Delta C_{2,2} = 0.026 \times 10^{-6}$ that are not included in the values for J_2 and $C_{2,2}$ in Tables 1 and 2. These corrections are small compared with the estimated uncertainties in J_2 and $C_{2,2}$.

The estimated gravity parameters for PJ1 and PJ2 separately and in combination are given in Tables 2 and S1 in the supporting information. The estimated values for the odd zonal harmonics, the sectoral and tesseral harmonics of degree and order 2, and the even zonal harmonics are well below the uncertainties so are not included in Table 2 except for J_3, $C_{2,2}$, and $S_{2,2}$ that are retained for comparison with previous experiments. The correlation factors between the gravity coefficients are given in Table S2 in the supporting information.

Table 2. Estimated Jovian Gravity Field Parameters From Juno's First Two Science Orbits Individually and in Combination[a]

Parameter	PJ1 Estimate	PJ2 Estimate	PJ1 and PJ2 Estimate
GM(km^3/s^2)	126,686,533.0 ± 2.0	126,686,533.0 ± 2.0	126,686,533.0 ± 2.0
J_2 ($\times 10^6$)	14,697.885 ± 1.918	14,696.496 ± 0.398	14,696.514 ± 0.272
J_3 ($\times 10^6$)			−0.067 ± 0.458
J_4 ($\times 10^6$)	−586.595 ± 0.554	−586.635 ± 0.314	−586.623 ± 0.363
J_6 ($\times 10^6$)	34.336 ± 0.352	34.246 ± 0.126	34.244 ± 0.236
J_8 ($\times 10^6$)	−2.468 ± 0.415	−2.482 ± 0.159	−2.502 ± 0.311
$C_{2,2}$ ($\times 10^6$)	0.072 ± 0.174	−0.007 ± 0.067	0.005 ± 0.170
$S_{2,2}$ ($\times 10^6$)	0.128 ± 0.153	−0.013 ± 0.055	−0.010 ± 0.214
α(deg)	268.058 ± 0.010	268.057 ± 0.002	268.057 ± 0.002
δ(deg)	64.490 ± 0.011	64.497 ± 0.003	64.496 ± 0.013

[a]The zonal harmonics J_n and degree 2 tesseral harmonics $S_{i,j}$ and $C_{i,j}$ are unnormalized and dimensionless. The Jupiter spin axis direction is given by right ascension α and declination δ at epoch J2000. The value and uncertainty for the Jupiter planet mass parameter (GM) for Juno analysis are taken from *Jacobson et al.* [1999].

The uncertainties listed account for both the effect of the observed data noise and from possible systematic errors using the consider analysis described above. The uncertainties include the effect of unestimated parameters describing a possible gravity field of degree and order 30 due to surface winds with depth of 10,000 km [*Parisi et al.*, 2016]. In that study the wind velocity observed at the cloud top was propagated downward along coaxial cylinders whose axes are parallel to the spin direction of Jupiter. This three-dimensional profile is then multiplied by a negative exponential function characterized by the folding scale *H*. Of the set of folding scales in that paper, we used the value of 10,000 km in the analysis here since that gave the largest values for gravity harmonic coefficients that cannot be well estimated by the Juno data. This results in gravity coefficient uncertainties that are fairly conservative but not an upper bound since the deeper winds may be larger. The only observation of Jovian wind speeds below the cloud levels, from the Galileo probe, showed significantly larger wind speed [*Atkinson et al.*, 1998]. The use of consider analysis affects the postfit covariance matrix but does not affect the estimated gravity field coefficients.

The estimated gravity coefficients from PJ1 and PJ2 separately agree within these uncertainties. This gives some confidence that there are no major sources of unidentified systematic errors. Note that the estimates from the combination of data from PJ1 and PJ2 are not simply a weighted average of the results from each arc separately. The combination of two arcs with different geometry relative to the Jovian surface and the direction to Earth, reduces the correlations between the parameters, particularly between the harmonic coefficients and the direction of the Jovian spin axis. This can result in an estimate slightly outside the estimates from the single-arc estimates. The coefficient uncertainties from the PJ2 solution are generally smaller than from the PJ1 solution, partly because of lower data noise for PJ2 and partly because the orbit normal for PJ2 is less aligned with the Earth-Jupiter direction giving a larger measured Doppler shift. The uncertainties

Table 3. Estimated Jovian Gravity Field Parameters From Pioneer and Voyager; From Pioneer and Voyager Combined With Galileo (Jup230); From Pioneer, Voyager, Galileo, Cassini, and New Horizons (Jup310); and From Juno's First Two Science Orbits in Combination[a]

Parameter	Pioneer/Voyager	Jup230	Jup310	Juno PJ1&PJ2
GM(km^3/s^2)	126,686,537.5 ± 101	126,686,534.9 ± 1.5	126,686,534.2 ± 2.7	126,686,533.0 ± 2.0
J_2 ($\times 10^6$)	14,697.3 ± 1	14,696.43 ± 0.21	14,695.62 ± 0.29	14696.514 ± 0.272
J_3 ($\times 10^6$)	1.4 ± 5	−0.64 ± 0.90		−0.067 ± 0.458
J_4 ($\times 10^6$)	−583.9 ± 5	−587.14 ± 1.68	−591.31 ± 2.06	−586.623 ± 0.363
J_6 ($\times 10^6$)	30.8 ± 20	34.25 ± 5.22	20.78 ± 4.87	34.244 ± 0.236
J_8 ($\times 10^6$)				−2.502 ± 0.311
$C_{2,2}$ ($\times 10^6$)	−0.030 ± 0.150	0.007 ± 0.008	−0.010 ± 0.067	0.005 ± 0.170
$S_{2,2}$ ($\times 10^6$)	−0.007 ± 0.150	−0.013 ± 0.009	−0.014 ± 0.061	−0.010 ± 0.214
α(deg)	268.058 ± 0.005	268.0566 ± 0.0002	268.0571 ± 0.0003	268.057 ± 0.002
δ (deg)	64.494 ± 0.002	64.4953 ± 0.0001	64.4958 ± 0.0001	64.496 ± 0.013

[a]The zonal harmonics J_n and degree 2 tesseral harmonics $S_{i,j}$ and $C_{i,j}$ are unnormalized and dimensionless. The Jupiter spin axis direction is given by right ascension α and declination δ at epoch J2000. The gravity harmonics from Pioneer and Voyager have been scaled from the Jupiter radius originally used to the radius 71,492 km and the pole direction converted from Earth mean equator of 1950 to Earth mean equator of 2000. The value and uncertainty for the Jupiter planet mass parameter (GM) for Juno analysis are taken from *Jacobson et al.* [1999].

for some coefficients for the solution with both PJ1 and PJ2 data are larger than the uncertainties for the solution with only PJ2 data. As mentioned earlier, this is a consequence of the consider analysis technique when there are significant correlations between estimated and considered (unestimated) parameters. We expect this effect to be smaller in the future when more Juno data are available.

The Juno gravity estimates are compared with earlier estimates in Table 3. The estimates from Pioneer and Voyager analysis are from *Campbell and Synnott* [1985], adjusted where necessary for difference in assumed radius and reference frame for the direction of the spin axis. Also shown in Table 3 are estimates derived from combination of the Pioneer and Voyager data with data from the Galileo mission [*Jacobson*, 2003] and also with data from the Cassini and New Horizons mission [*Jacobson*, 2009]. These are associated with ephemerides for the Jovian satellites designated Jup230 and Jup310. Unlike the Juno results presented here and the earlier estimates by *Campbell and Synnott* [1985], the uncertainties for Jup230 and Jup310 do not account for possible systematic errors. The uncertainties for the Juno data ignoring systematic errors are about 1 order of magnitude smaller than the uncertainties given here. Aside from the differences in development of uncertainties, the estimated coefficients are generally in agreement within uncertainties. The uncertainties in J_4 and J_6, that are key parameters for constraining Jovian interior models, are improved with the Juno data over earlier estimates by factors of 4.6 and 22, respectively. The estimated J_4 and J_6 from the Jup310 solution are significantly different from the other solutions. This is thought to be due to systematic errors in photographic observations of Amalthea by Cassini and New Horizons.

5. Discussion

The improved estimates of the even zonal harmonics provide better constraints on models of the Jovian interior. Some previously published interior models, characterized by different temperature, composition, and core mass and size, are close to agreement with the estimated zonal harmonics J_4 and J_6 within uncertainties [e.g., *Nettelmann et al.*, 2012; *Miguel et al.*, 2016] while others are not [e.g., *Hubbard and Militzer*, 2016]. While Jupiter interior models can be adjusted to fit the Juno estimates [e.g., *Wahl et al.*, 2017], it is possible that differential rotation can produce a change to J_4 and J_6 expected for a uniformly rotating Jupiter that can affect their interpretation [e.g., *Hubbard*, 1982]. Differential rotation might also lead to small nonzero values of the odd zonal harmonics [*Kaspi*, 2013]. From only two perijoves no clear signature of differential rotation has been detected. Future Juno science orbits are expected to provide significantly improved estimates of the Jovian gravity field that will either detect or tightly constrain effects due to differential rotation.

Acknowledgments
We thank the Juno gravity science processing team, Oscar Yang, Daniel Kahan, Meegyeong Paik, and Elias Barbinis, and the Juno operations team. The research described in this paper was carried out at the Jet Propulsion Laboratory, California Institute of Technology, under a contract with the National Aeronautics and Space Administration; by the Southwest Research Institute under contract with the National Aeronautics and Space Administration; and by the Sapienza University of Rome, University of Bologna, and University of Pisa under the sponsorship of the Italian Space Agency. The data used in this paper are available through the NASA Planetary Data System (to be posted on June 2017).

References

Anderson, J. D., G. W. Null, and S. K. Wong (1974), Gravity results from Pioneer 10 Doppler data, *J. Geophys. Res.*, *79*, 3661–3664.
Asmar, S. W., J. W. Armstrong, L. Iess, and P. Tortora (2005), Spacecraft Doppler tracking: Noise budget and accuracy achievable in precision radio science observations, *Radio Sci.*, *40*, RS2001, doi:10.1029/2004RS003101.
Atkinson, D. H., J. B. Pollack, and A. Seiff (1998), The Galileo probe Doppler wind experiment: Measurement of the deep zonal winds on Jupiter, *J. Geophys. Res.*, *103*, 22,911–22,928.
Barnes, J. A., et al. (1971), Characterization of frequency stability, *IEEE Trans. Instrum. Meas.*, *1001*, 105–120.
Bierman, G. (1977), *Factorization Methods for Discrete Sequential Estimation*, chap. 8, pp. 162–182, Academic Press, New York.
Bird, M. K., S. W. Asmar, J. P. Brenkle, P. Edenhofer, O. Funke, M. Pätzold, and H. Volland (1992), Ulysses radio occultation observations of the Io plasma torus during the Jupiter encounter, *Science*, *257*, 1531–1535.
Campbell, J. K., and S. P. Synnott (1985), Gravity field of the Jovian system from Pioneer and Voyager tracking data, *Astron. J.*, *90*, 364–372.
Eshleman, V. R., G. L. Tyler, G. E. Wood, G. F. Lindal, J. D. Anderson, G. S. Levy, and T. A. Croft (1979), Radio science with Voyager at Jupiter: Initial Voyager 2 results and a Voyager 1 measure of the Io Torus, *Science*, *206*, 959–962.
Gavrilov, S. V., and V. N. Zharkov (1977), Love numbers of the giant planets, *Icarus*, *32*, 443–449.
Hubbard, W. B. (1982), Effects of differential rotation on the gravitational figures of Jupiter and Saturn, *Icarus*, *52*, 509–515.
Hubbard, W. B., and B. Militzer (2016), A preliminary Jupiter model, *Astrophys. J.*, *820*, 80, doi:10.3847/0004-637X/820/1/80.
Jacobson, R., R. Haw, T. McElrath, and P. Antreasian (1999), A comprehensive orbit reconstruction for the Galileo prime mission in the J2000 system, *Adv. Astronaut. Sci.*, *103*, 465–486.
Jacobson, R. A. (2003), Jupiter satellite ephemeris file Jup230, NASA Navigation and Ancillary Information Facility. [Available at https://naif.jpl.nasa.gov/pub/naif/generic_kernels/spk/satellites/a_old_versions/jup230l.cmt.]
Jacobson, R. A. (2009), Jupiter satellite ephemeris file Jup310, NASA Navigation and Ancillary Information Facility. [Available at https://naif.jpl.nasa.gov/pub/naif/generic_kernels/spk/satellites/jup310.cmt.]
Kaspi, Y. (2013), Inferring the depth of the zonal jets on Jupiter and Saturn from odd gravity harmonics, *Geophys. Res. Lett.*, *40*, 676–680, doi:10.1029/2012GL053873.
Kaula, W. M. (1966), *Introduction to Satellite Geodesy*, chap. 1, pp. 1–11, Blaisdell, Waltham, Mass.
Keihm, S. J., A. Tanner, and H. Rosenberger (2004), Measurements and calibration of tropospheric delay at goldstone from the Cassini media calibration system, *Interplanet. Network Prog. Rep.*, *42-158*, 1–17.

Lindal, G. F., et al. (1981), The atmosphere of Jupiter: An analysis of the Voyager radio occultation measurements, *J. Geophys. Res.*, *86*, 8721–8727.

Miguel, Y., T. Guillot, and L. Fayon (2016), Jupiter internal structure: The effect of different equations of state, *Astron. Astrophy.*, *596*, 12, doi:10.1051/0004-6361/201629732.

Milani, A., and G. Gronchi (2010), *Theory of Orbit Determination*, chap. 15, pp. 311–322, Cambridge Univ. Press.

Nettelmann, N., A. Becker, B. Holst, and R. Redmer (2012), Jupiter models with improved ab initio hydrogen equation of state (H-Reos.2), *Astrophys. J.*, *750*(1), 52, doi:10.1088/0004-637X/750/1/52.

Null, G. W., J. D. Anderson, and S. K. Wong (1975), Gravity field of Jupiter from Pioneer 11 tracking data, *Science*, *188*, 476–477.

Parisi, M., E. Galanti, S. Finocchiaro, L. less, and Y. Kaspi (2016), Probing the depth of Jupiter's Great Red Spot with the Juno gravity experiment, *Icarus*, *267*, 232–242.

Wahl, S. M., W. B. Hubbard, B. Militzer, T. Guillot, Y. Miguel, Y. Kaspi, R. Helled, D. Reese, N. Movshovitz, and E. Galanti (2017), Comparing Jupiter interior structure models to Juno gravity measurements and the role of an expanded core, *Geophys. Res. Lett.*, doi:10.1002/2017GL073160, in press.

Woo, R., F.-C. Yang, K. W. Yip, and W. B. Kendall (1976), Measurements of large-scale density fluctuations in the solar wind using dual-frequency phase scintillations, *Astrophys. J.*, *210*, 568–574.